# ChemComm

Check for updates

## 5,5′-Biindeno[2,1-c]fluorene: importance of C5–C5′ linkage for an indeno[2,1-c]fluorene dimer exhibiting an open-shell ground state†

Neha Maurya, [ID] [a] Palash Jana, [b] Himanshu Sharma, [ID] [a] Subhajit Bandyopadhyay [b] and Soumyajit Das [ID] *[a]

Mesityl-protected indeno[2,1-c]fluorene and its C2–C2′-linked dimer 2,2′-biindeno[2,1-c]fluorene are closed-shell molecules. Herein, we report the synthesis and characterization of a mesityl-protected 5,5′-biindeno[2,1-c]fluorene displaying 26.4% diradical and 0.9% tetraradical characters. The C5–C5′ linkage between two [2,1-c]IFs is crucial for its open-shell character, resulting in its far-red UV-vis absorption, redox amphoterism, partially *para*-quinoidal *as*-indacene core, and temperature-dependent EPR response due to a small singlet–triplet energy gap.

Formally, antiaromatic parent indeno[2,1-c]fluorene (Fig. 1a) is an open-shell (OS) diradicaloid polycyclic hydrocarbon (PH) with the weakest diradical character index ($y_0 = 0.021$)[1] among the five indenofluorene (IF) isomers.[2] The 5,8-disubstitution of [2,1-c]IF by bulky aryl (like mesityl for **1**) or ethynyl groups is proven to be an effective approach to isolate sterically protected stable [2,1-c]IF derivatives,[2d,3] but these are closed-shell (CS) quinoidal PHs. Symmetric[2d] and unsymmetric[3b] helical [2,1-c]IF derivatives usually have very small *P/M*-inversion barriers unless helically π-extended,[4] a promising strategy to develop chiral diradicaloids with potential chiroptical properties.[4b] The curved shape of [2,1-c]IF was utilized to construct unique PHs, such as a helical monoradical,[5] a macrocyclic tetraradicaloid,[6] indaceno-difluorene derivatives,[3a,4a] and benzo-extended [2,1-c]IFs[7] with tunable antiaromaticity. From an application viewpoint, IF **1** was employed in bulk-heterojunctions[8] as an electron-acceptor and recently our group found it to be an ambipolar charge carrier with balanced hole and electron mobilities in the order of $10^{-3}$ cm$^2$ V$^{-1}$ s$^{-1}$.[3b] Additionally, the potential of IFs for application in non-linear optics[9] and a recent report on IF-based PHs in
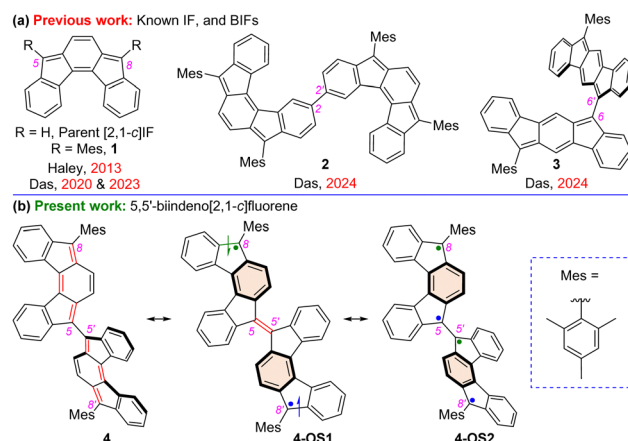


Fig. 1 (a) Antiaromatic indeno[2,1-c]fluorene **1**, our reported 2,2′-bi-indeno[2,1-c]fluorene **2**, and 6,6′-biindeno[1,2-b]fluorene **3**. (b) Closed-shell structure **4** for the targeted mesityl disubstituted 5,5′-biindeno[2,1-c]-fluorene, and its open-shell diradical and tetraradical resonance forms **4-OS1** and **4-OS2**, respectively.

single-molecule conductance[10] studies suggested that IF derivatives with an OS ground state could be potential organic spintronics materials, tempting us to explore new IF-based polycyclic antiaromatic hydrocarbons with an OS ground state.

Dimerization of **1** by carbons 2 and 2′ resulted in an IF dimer 2,2′-biindeno[2,1-c]fluorene **2** with a smaller energy gap between the highest occupied and lowest unoccupied molecular orbitals (HOMO and LUMO) in comparison to monomer **1**.[11] Although a small HOMO–LUMO gap (henceforth denoted as HLG) is the usual criterion for displaying OS properties,[12] BIF **2** did not show an OS ground state, likely due to a large singlet(S)–triplet(T) energy gap ($\Delta E_{S-T} = -13.25$ kcal mol$^{-1}$). Very recently, we reported the synthesis of 6,6′-[1,2-b]BIF **3** as an OS IF dimer with a $y_0$ of 0.268 and a tetraradical character index ($y_1$) of 0.007.[13] Dimerizing two indeno[1,2-b]fluorene monomers by carbons 6 and 6′ bearing large HOMO and LUMO distributions resulted in a decrease in HLG and S–T gap ($\Delta E_{S-T} = -4.85$ kcal mol$^{-1}$) for **3** compared to those of known 3,3′-linked [1,2-b]BIF.[11] Therefore,

*[a] Department of Chemistry, Indian Institute of Technology Ropar, Rupnagar 140001, Punjab, India. E-mail: chmsdas@iitrpr.ac.in*

*[b] Department of Chemical Sciences, Indian Institute of Science Education and Research (IISER) Kolkata, Mohanpur 741246, West Bengal, India*
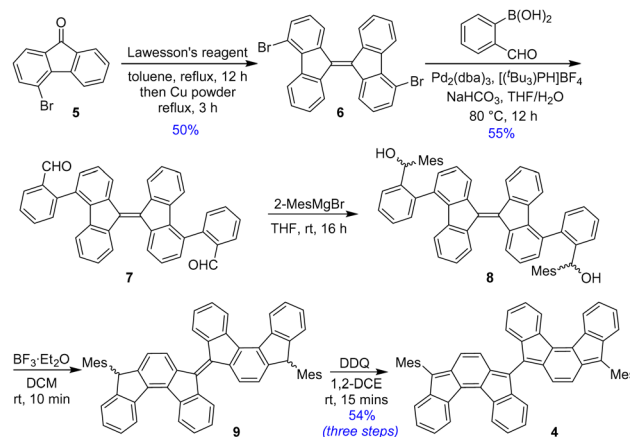
connecting two [2,1-*c*]IF units by the non-bridgehead (apical) carbons 5 and 5′ bearing larger HOMO and LUMO coefficients[3b] than the C2 and C2′ positions is envisaged to significantly tune the ground-state properties for 5,5′-biindeno[2,1-*c*]fluorene **4** (Fig. 1b) by further compressing the HLG and $\Delta E_{S-T}$ compared to those of **2**. Herein, we report a facile synthesis for the newly designed BIF **4** that can be represented in three ground-state canonical structures: CS quinoidal **4**, diradicaloid **4-OS1**, and tetraradicaloid **4-OS2**. The ground state of **4** was systematically investigated by various analytical techniques, with the support of density functional theory (DFT) calculations.

As parent [2,1-*c*]IF possesses the weakest $y_0$ among the IF isomers,[1] we performed DFT studies at the (U)CAM-B3LYP/6-31G(d,p) level of theory[14] to examine the electronic ground state of BIF **4**. Compound **4** was found to have an OS singlet ground state with a small $\Delta E_{S-T} = -4.07$ kcal mol$^{-1}$, including a modest $y_0 = 0.264$ and a minor $y_1 = 0.009$, as estimated from the natural orbital occupancy numbers (NOON). The spin densities are delocalized across the entire molecule, with the larger Mulliken spin density values of 0.53 and 0.47 at the apical carbons 8/8′ and 5/5′, respectively (Fig. 2a). The frontier molecular orbital (FMO) profiles of the singly occupied molecular orbitals (SOMO) reveal a typical disjointed nature of the alpha (SOMO-α) and beta (SOMO-β) spins of **4** (Fig. 2b and c). Based on the computations, BIF **4** is expected to exhibit an OS singlet ground state with a smaller $\Delta E_{S-T}$ than that of **3**, while the OS characters are found to be identical to those of **3**.[13] A modest $y_0$ and an incredibly low $y_1$ indicate that the two radicals in **4-OS2** at the 5,5′-linkage may couple to form a bond, suggesting the contribution of **4-OS1** is more important.

The synthesis of BIF **4** is shown in Scheme 1. Dimerization of 4-bromo-9-fluorenone[15] **5** by Lawesson's reagent afforded 4,4′-dibromo-9,9′-bifluorenylidene **6** as *E/Z*-diastereomers. Treating diastereomeric mixture **6** with (2-formylphenyl)-boronic acid under Suzuki reaction condition gave dialdehyde **7** in 55% yield as a mixture of stereoisomers. The stereoisomeric mixture **7** was treated with an excess of 2-mesitylmagnesium bromide (2-MesMgBr) under ambient conditions to produce diol **8**. Crude **8** was reacted with BF$_3$·Et$_2$O to afford the dihydro precursor **9**. As partial formation of **4** was experienced in thin layer chromatography during the conversion of **8** to **9**, crude **9**

**Scheme 1** Synthesis of [2,1-*c*]IF dimer **4**.

was oxidatively dehydrogenated by 2,3-dichloro-5,6-dicyano-1,4-benzoquinone (DDQ) in 1,2-dichloroethane to produce desired BIF **4** as a greenish-black solid in 54% yield over three steps after column chromatographic purification. Nuclear magnetic resonance (NMR), high-resolution mass spectrometry (HRMS), and single crystal X-ray diffraction (SCXRD) analyses unequivocally confirmed the formation of BIF **4**.

Single crystals of BIF **4** (Fig. 3a), obtained by slow diffusion of acetonitrile into hexane solution, are found to pack in either slightly helical *P–P* linked or *M–M* linked homodimeric arrangement (Fig. 3b), presumably due to a low *P/M*-inversion barrier for [2,1-*c*]IF.[2d,3b] Two [2,1-*c*]IF units of BIF **4** form a torsional angle of ∼37.9°, which is smaller than that observed for BIF **3**.[13] A reduced torsional angle between two [2,1-*c*]IF units, which are linked *via* carbons 5 and 5′ with large orbital coefficients for HOMO and LUMO,[3b] suggests the possibility of greater

**Fig. 3** (a) X-ray crystallographic structure of **4** with the ellipsoids drawn at 30% probability level (hydrogens omitted), including NICS($\mathbf{1}$)$_{zz}$ (blue) and HOMA (green) values. (b) *P–P* and *M–M* linked homodimers of **4** in crystal packing. (c) EPR spectra of powder **4** recorded at variable temperatures (VT-EPR).
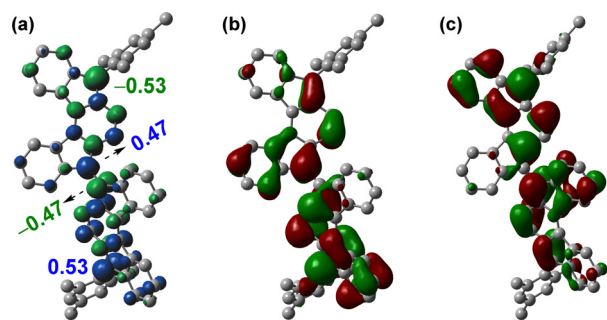
**Fig. 2** (a) Spin density distribution in **4**. Isovalue for surfaces: MO = 0.02, density = 0.005; frontier molecular orbitals of the (b) α-spin and (c) β-spin of **4**.
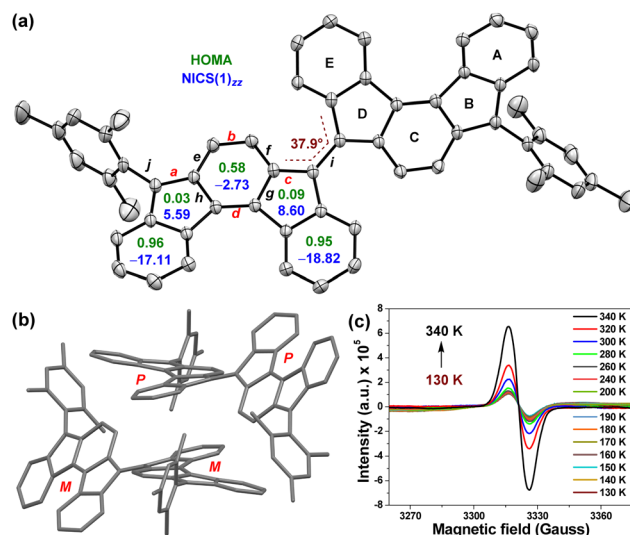
π-electronic communication between the IF units as the large C=C/C–C bond alternation in *para*-quinodimethane[16] (*p*-QDM) subunit of *as*-indacene[2d,3b] forms a polyene-like[13] π-conjugation path (shown in red for **4** in Fig. 1b). As a result, the C=C double and C–C single bond lengths of the *p*-QDM subunit are expected to be increased and decreased, respectively.[13]

The bond lengths (labelled *a* to *j* in Fig. 3a) determined from SCXRD and DFT analyses are summarized in Table 1 (see Fig. S12, ESI† for complete bond length analyses, including e.s.d. values), and compared with the SCXRD data of **1**.[2d] Our analyses found that *exo*-methylene C=C double bonds *a* (1.377 Å; DFT: 1.396 Å) and *c* (1.393 Å; DFT: 1.419 Å) are longer than those of **1** (Table 1 and Fig. S4, ESI†); in particular, the length of *c* is similar to **3**, but bonds *b* and *d* are identical in length to those of **1** by SCXRD analysis. C–C single bonds *e*–*h* of the central benzenoid ring are relatively shorter than those of **1**. Furthermore, C–C single bond *i* that links two IF units is 1.451 Å (DFT: 1.421 Å), which is shorter than C–C single bond *j* (1.484 Å; DFT: 1.480 Å) linking the mesityl group to the [2,1-*c*]IF core and identical to that in BIF **3** (1.452 Å),[13] suggesting the gain of of a partial double bond character for bond *i* due to efficient delocalization of π-electrons between two [2,1-*c*]IF units. Although the X-ray structure of **2** is unavailable, the DFT data also suggest a greater π-bond character for C5–C5′ bond *i* in **4** than that of the C2–C2′ bond in **2** (1.481 Å, Table S4, ESI†).[11] While longer C=C bonds *c* and *a*, and shorter C–C bond *i* suggest the contribution of a bifluorenylidene-type[13,17] diradical form **4-OS1** in the ground state, the short C=C bonds *b* and *d* indicate the presence of fairly *p*-quinoidal CS form **4**. We attribute such observation in BIF **4** to a room-temperature (rt)-accessible low-lying CS state, which is computed to be only 1.88 kcal mol$^{-1}$ (Table S1, ESI†) higher in energy than the OS singlet ground state; a phenomenon that is comparable to the IF derivative exhibiting low OS character.[12b]

Electron paramagnetic resonance (EPR) spectroscopy confirmed the OS behaviour of **4**. As shown in Fig. 3c, the powder sample of **4** displayed a characteristic broad EPR signal at 340 K. As the temperature was lowered, the signal intensity decreased due to reduced population of paramagnetic triplet species at lower temperatures (Fig. 3c), confirming an OS singlet ground state. A careful fitting of the EPR data using the Bleaney–Bowers equation[18] gave an experimental

$\Delta E_{S-T} = -4.12 \pm 0.26$ kcal mol$^{-1}$ (Fig. S14, ESI†), which closely matches the theoretical value. The harmonic oscillator model for aromaticity (HOMA, Fig. 3a)[19] analysis of optimized structure **4** indicated aromaticity for rings A (0.96) and E (0.95) as these rings displayed insignificant bond length alternation (BLA).[20] Rings B (0.03) and D (0.09) are essentially nonaromatic as they showed large BLA (Fig. 3a), whereas central benzenoid ring C exhibits a relatively small BLA (0.58), suggesting its weak aromaticity. Nucleus independent chemical shift[21] [NICS(1)$_{zz}$, Fig. 3a] values for **4** are in line with the HOMA values, suggesting greater aromaticity for rings A ($-17.11$) and E ($-18.82$), while ring C is weakly aromatic ($-2.73$). Rings B (5.59) and D (8.60) exhibit weak antiaromatic character. The geometrical and magnetic criteria of aromaticity analyses are in agreement with the X-ray analysis, suggesting that the OS form of **4** partly contributes to the singlet ground state.

The electronic absorption spectrum of dark-green-colored **4** (Fig. 4a) in chloroform showed several high-energy absorption bands in the UV-vis region including a broad and intense band in the far-red region ($\lambda_{max} = 720$ nm, $\varepsilon = 16\,200$ M$^{-1}$ cm$^{-1}$) that accompanies a shoulder at 785 nm and extends to 935 nm in the near-IR region. The lowest energy absorption band originates from the HOMO → LUMO and HOMO−1 → LUMO+1 transitions, as per the time-dependent-DFT calculations (TD-DFT: $\lambda_{max(TD)} = 644.9$ nm, oscillator strength ($f$) = 0.6203, Table S2, ESI†). The lowest energy wavelength maximum of BIF **4** was found to be red-shifted by 88 nm compared to that of BIF **2**, clearly indicating greater electronic communication in **4**, which is also evident from the higher molar absorptivity ($\varepsilon$). The optical HLG of **4** was roughly estimated to be 1.33 eV from the absorption edge, which is approximately 0.17 eV smaller than those of BIF **2** and **3**. Like compounds **1–3**, BIF **4** was also found to be non-emissive to the naked eye. It has a half-life of around 2.7 days in toluene under ambient light and temperature in air (Fig. S13, ESI†), suggesting relatively less stability than **3**. However, **4** was stable as a solid for several months when stored in a freezer.

The electrochemical behavior of **4** was studied by cyclic voltammetry (CV) and differential pulse voltammetry (DPV) in dichloromethane using Bu$_4$NPF$_6$ as electrolyte. It displays four-stage redox amphoterism (Fig. 4b) with two reversible reduction waves at half-wave potentials $E_{1/2}^{red1} = -1.28$ V and $E_{1/2}^{red1} = -1.50$ V, and two reversible oxidation waves at $E_{1/2}^{red1} = 0.30$ V and $E_{1/2}^{red1} = 0.61$ V (*vs.* ferrocene/ferrocenium (Fc/Fc$^+$)).

**Table 1**  Comparison of mean C–C bond lengths (Å) of **4** and **1**

| Bonds[a] | **4**[b] | **4**[c] | **1**[d] |
|---|---|---|---|
| *a* | 1.377 | 1.396 | 1.371 |
| *b* | 1.354 | 1.368 | 1.357 |
| *c* | 1.393 | 1.419 | 1.374 |
| *d* | 1.367 | 1.376 | 1.366 |
| *e* | 1.431 | 1.417 | 1.434 |
| *f* | 1.432 | 1.417 | 1.434 |
| *g* | 1.465 | 1.447 | 1.470 |
| *h* | 1.466 | 1.451 | 1.470 |
| *i* | 1.451 | 1.421 | — |
| *j* | 1.484 | 1.480 | 1.486 |

[a] Bonds *a*–*j* are labelled in Fig. 3a. [b] SCXRD data. [c] DFT data. [d] SCXRD data from ref. 2d.
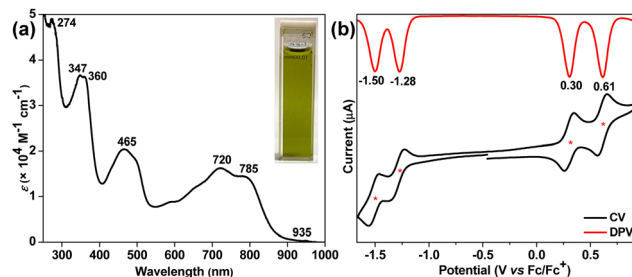


**Fig. 4**  (a) UV–vis–NIR spectrum of **4** in chloroform. (b) CV and DPV of **4** in DCM.

The HOMO and LUMO energy levels of **4** were −4.98 eV and −3.65 eV, respectively, as measured from the onset oxidation and reduction potentials. The electrochemical HLG is 1.33 eV for **4**, which is 0.29 eV and 0.05 eV smaller than those of **2** and **3**, respectively. Notably, both HOMO and LUMO energies of **4** are destabilized in comparison to **3**. Importantly, the greater destabilization of the HOMO level for BIF **4** makes it more susceptible to oxidative degradation in air compared to isomeric BIF **3**, which is evidenced by the photostability test.

The larger HOMO and LUMO coefficients on the C5/C8 position of **1**, relative to C2/C11, suggest that attaching an ambipolar [2,1-*c*]IF unit[3b] to the C5 position of another [2,1-*c*]IF scaffold should influence the HOMO and LUMO energies more than it could do for C2 substitution. Indeed, **4** has more destabilized HOMO and stabilized LUMO levels than those of **2** (Table S6, ESI†).[11] Thus, **4** exhibits a smaller HLG than **2**, which is crucial[12,13] for exhibiting OS properties as a triplet excited state is pushed[12b] toward the singlet ground state. The SCXRD data of **4** indicate the presence of a moderately quinoidal *p*-QDM subunit in the IF core, while VT-EPR confirms a singlet OS ground state, which is in line with computations suggesting the OS singlet state of **4** to be slightly more stable than the CS state. Structurally, BIF **2** is CS with a strong *p*-quinoidal core as it gains no extra aromatic stabilization in its π-extended OS form (Fig. S15, ESI†). However, BIF **4** restores two additional Clar sextets[13,22] in diradical form **4-OS1**, but has no major driving force toward **4-OS2**. Overall, a modest OS character and the presence of a moderately *p*-quinoidal IF core due to a low-lying CS state suggest the partial contribution of the quinoidal form of **4** to the OS ground state alongside **4-OS1**.

In summary, the synthesis and characterization of a novel BIF **4** suggest that linking two [2,1-*c*]IF units by C5 and C5′ positions, instead of C2 and C2′ positions, can remarkably tune the electronic ground state. A small dihedral angle due to C5–C5′ linkage between two IFs extends the π-delocalization path, resulting in smaller HLG and $\Delta E_{\text{S-T}}$ for **4** than for known BIFs. BIF **4** may be viewed as a desymmetrized [2,1-*c*]IF due to the attachment of electronically different aryls ([2,1-*c*]IF/Mes) at C5/C8 positions, resulting in an OS ground state with a low-lying CS state. Though the OS character of [2,1-*c*]IF is too weak[1] to be detected experimentally for **1**,[2d,3] it is now observable by EPR and SCXRD analyses for **4** and supported by DFT calculations. The fullerene-$C_{60}$ fragment [2,1-*c*]IF can act as an electron-accepting scaffold in a bulk-heterojunction device,[8] while the high HOMO of [2,1-*c*]IF dimer **4** suggests its ability as a donor for organic electronics.

## Data availability

The data supporting the findings are available in the ESI.†

## Conflicts of interest

There are no conflicts to declare.

## Notes and references

1 K. Fukuda, T. Nagami, J. Fujiyoshi and M. Nakano, *J. Phys. Chem. A*, 2015, **119**, 10620.
2 (a) D. T. Chase, B. D. Rose, S. P. McClintock, L. N. Zakharov and M. M. Haley, *Angew. Chem., Int. Ed.*, 2011, **50**, 1127; (b) A. Shimizu and Y. Tobe, *Angew. Chem., Int. Ed.*, 2011, **50**, 6906; (c) A. Shimizu, R. Kishi, M. Nakano, D. Shiomi, K. Sato, T. Takui, I. Hisaki, M. Miyata and Y. Tobe, *Angew. Chem., Int. Ed.*, 2013, **52**, 6076; (d) A. G. Fix, P. E. Deal, C. L. Vonnegut, B. D. Rose, L. N. Zakharov and M. M. Haley, *Org. Lett.*, 2013, **15**, 1362; (e) J. J. Dressler, Z. Zhou, J. L. Marshall, R. Kishi, S. Takamuku, Z. Wei, S. N. Spisak, M. Nakano, M. A. Petrukhina and M. M. Haley, *Angew. Chem., Int. Ed.*, 2017, **56**, 15363.
3 (a) H. Sharma, P. K. Sharma and S. Das, *Chem. Commun.*, 2020, **56**, 11319; (b) H. Sharma, A. Ankita, P. Bhardwaj, U. K. Pandey and S. Das, *Org. Mater.*, 2023, **5**, 72.
4 (a) Q. Jiang, Y. Han, Y. Zou, H. Phan, L. Yuan, T. S. Herng, J. Ding and C. Chi, *Chem. – Eur. J.*, 2020, **26**, 15613; (b) Á. Martínez-Pinel, L. Lezama, J. M. Cuerva, R. Casares, V. Blanco, C. M. Cruz and A. Millán, *Org. Lett.*, 2024, **26**, 6012; (c) E. Sidler, R. Hein, D. Doellerer and B. L. Feringa, *J. Am. Chem. Soc.*, 2024, **146**, 19168.
5 S. Herzog, A. Hinz, F. Breher and J. Podlech, *Org. Biomol. Chem.*, 2022, **20**, 2873.
6 S. Nobusue, H. Miyoshi, A. Shimizu, I. Hisaki, K. Fukuda, M. Nakano and Y. Tobe, *Angew. Chem., Int. Ed.*, 2015, **54**, 2090.
7 T. Jousselin-Oba, P. E. Deal, A. G. Fix, C. K. Frederickson, C. L. Vonnegut, A. Yassar, L. N. Zakharov, M. Frigoli and M. M. Haley, *Chem. – Asian J.*, 2019, **14**, 1737.
8 K. Paudel, B. Johnson, M. Thieme, M. M. Haley, M. M. Payne, J. E. Anthony and O. Ostroverkhova, *Appl. Phys. Lett.*, 2014, **105**, 043301.
9 S. Thomas and K. S. Kim, *Phys. Chem. Chem. Phys.*, 2014, **16**, 24592.
10 (a) R. Casares, Á. Martínez-Pinel, S. Rodríguez-González, I. R. Márquez, L. Lezama, M. T. González, E. Leary, V. Blanco, J. G. Fallaque, C. Díaz, F. Martín, J. M. Cuerva and A. Millán, *J. Mater. Chem. C*, 2022, **10**, 11775; (b) R. Casares, S. Rodríguez-González, Á. Martínez-Pinel, I. R. Márquez, M. T. González, C. Díaz, F. Martín, J. M. Cuerva, E. Leary and A. Millán, *J. Am. Chem. Soc.*, 2024, **146**, 29977.
11 H. Sharma, Ankita, V. Mittal, U. K. Pandey and S. Das, *Org. Lett.*, 2024, **26**, 2617.
12 (a) S. Das and J. Wu, *Phys. Sci. Rev.*, 2017, **2**, 20160109; (b) P. K. Sharma, P. Jana, S. Bandyopadhyay and S. Das, *Chem. Commun.*, 2024, **60**, 7319.
13 H. Sharma, P. Jana, D. Mallick, S. Bandyopadhyay and S. Das, *Chem. Sci.*, 2024, **15**, 20215.
14 I. Casademont-Reig, E. Ramos-Cordoba, M. Torrent-Sucarrat and E. Matito, *Molecules*, 2020, **25**, 711.
15 S. Thiery, D. Tondelier, C. Declairieux, B. Geffroy, O. Jeannin, R. Métivier, J. Rault-Berthelot and C. Poriel, *J. Phys. Chem. C*, 2015, **119**, 5790.
16 S. Das, S. Lee, M. Son, X. Zhu, W. Zhang, B. Zheng, P. Hu, Z. Zeng, Z. Sun, W. Zeng, R. Li, K. Huang, J. Ding, D. Kim and J. Wu, *Chem. – Eur. J.*, 2014, **20**, 11410.
17 Y. Ishigaki, T. Harimoto, T. Shimajiri and T. Suzuki, *Chem. Rev.*, 2023, **123**, 13952.
18 B. Bleaney and K. D. Bowers, *Proc. R. Soc. London, Ser. A*, 1952, **214**, 451.
19 T. Lu and F. Chen, *J. Comput. Chem.*, 2012, **33**, 580.
20 H. Sharma, N. Bhardwaj and S. Das, *Org. Biomol. Chem.*, 2022, **20**, 8071.
21 H. Fallah-Bagher-Shaidaei, C. S. Wannere, C. Corminboeuf, R. Puchta and P. V. R. Schleyer, *Org. Lett.*, 2006, **8**, 863.
22 (a) P. Yadav, S. Das, H. Phan, T. S. Herng, J. Ding and J. Wu, *Org. Lett.*, 2016, **18**, 2886; (b) Z. Zeng, X. Shi, C. Chi, J. T. L. Navarrete, J. Casado and J. Wu, *Chem. Soc. Rev.*, 2015, **44**, 6578.